Electronic Supplementary Material (ESI) for Journal of Materials Chemistry A.

An Electrochromic Supercapacitor and Its Hybrid Derivatives: Quantifiably Determining Their Electrical Energy Storage by an Optical Measurement

Electronic Supplementary Information

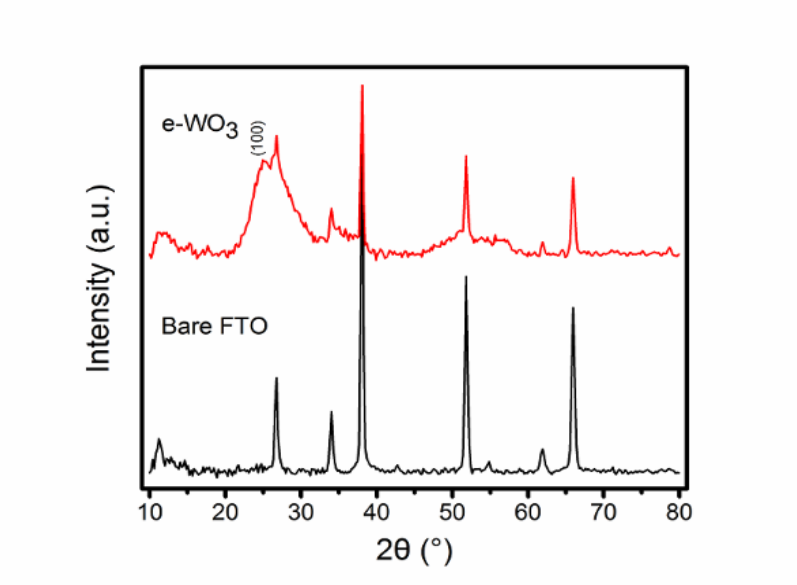

Figure S1. XRD patterns of e-WO_3 and bare FTO.

Figure S1 shows the XRD patterns of e-WO_3 on the FTO coated glass (red line) and bare FTO coated glass (black line). Obviously, the XRD patterns of e-WO_3 on the FTO coated glass contains the broad peaks and some additional sharp peaks. These features correspond to the unique structure of e-WO_3 particles – small crystals embedded in the amorphous matrix. In addition, the most intensive peak (2θ=24°) in XRD patterns of e-WO_3 can be identified as the (001) face of the tungsten oxide with the cubic phase (JCPDS no. 41-0905, cubic, Pm/3m).

Table S1. Electrical energy storage (EES) obtained from the ideal and tested galvanostatic curves and their differences.

EES from ideal curve	EES from tested curve		Differences	
	Charging	Discharging	Charging	Discharging
20%	17.12%	26.91%	2.88%	6.91%
40%	41.86%	52.12%	1.86%	12.12%
60%	67.02%	76.27%	7.02%	16.27%
80%	89.43%	94.07%	9.43%	14.07%

Table S1 lists the electrical energy storage (EES) obtained from the ideal curves and real tested curves. Evidently, deviations from the ideal curve at any EES can be found in this table. Furthermore, the deviation can reach as large as 16.27% at the EES=60% during the discharging process.

Table S2. Comparison of capacitance of electrochromic supercapacitors based on WO_3.

Electrode configuration	Electrolyte	Specific capacitance	Ref.
e-WO_3	PVA/H_2SO_4	3.5 mF cm^{-2} (device) 7 mF cm^{-2} (electrode)	This work
e-WO_3//PPy	PVA/H_2SO_4	20 mF cm^{-2} (device) 40 mF cm^{-2} (electrode)	
e-WO_3//MnO_2	PVA/H_2SO_4	45 mF cm^{-2} (device) 90 mF cm^{-2} (electrode)	
$W_{18}O_{49}$//PANI	1M H_2SO_4	10 mF cm^{-2}	1
WO_3//PANI	0.5M H_2SO_4	12 mF cm^{-2}	2
WO_3	0.5M H_2SO_4	12.8 mF cm^{-2}	3
$WO_3 \cdot 2H_2O$	PVA/H_2SO_4	22 mF cm^{-2}	4

From Table S2, it can be clearly seen that the performance of our supercapcitors is comparable to all other electrochromic supercapcitors based on WO3. Moreover, the hybrid electrochromic supercapacitors in our work shows very impressive capacitance, which strongly supports that high capacitance can be achieved by incorporating active materials with good capacitance to the WO_3 electrochromic supercapacitor without compromising the ability of indicating EES.

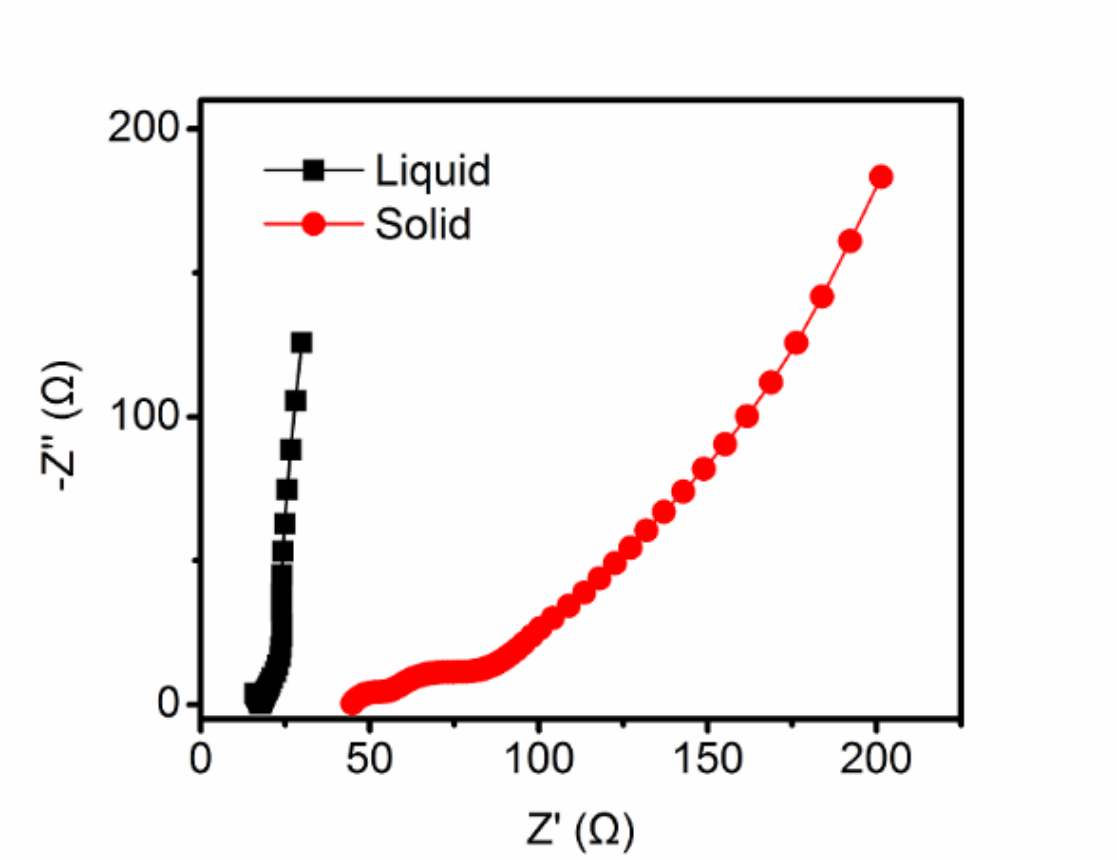

Figure S2. Nyquist plot of the e-WO_3 electrode tested in liquid and solid electrolyte.

It can be clearly seen from the Nyquist plot that the bulk resistance of electrode tested in liquid electrolyte is much smaller than that tested in solid electrolyte. This may be the result of the better contact of active materials and electrolyte in liquid than that in solid electrolyte. Moreover, the capacitive behavior is much sluggish when the e-WO_3 is tested in the solid electrolyte. These two factors may damage the performance of the solid-state electrochromic supercapcitors as can been seen from Figure 3, showing that the performance of e-WO_3 based electrode in liquid electrolyte is better than that in solid electrolyte.

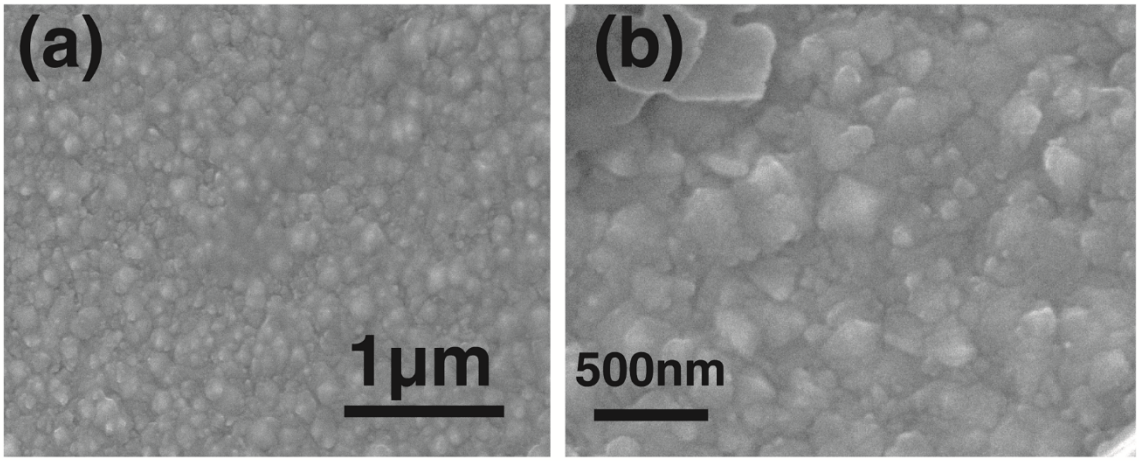

Figure S3. (a) SEM images of the e-WO3 electrode after 100 electrochromic and electrochemical cycles, and (b) higher magnification SEM image of the electrode.

Compared with the SEM images before the electrochromic and electrochemical process in Figure 2a, no significant difference can be found. This indicates that e-WO_3 is proper for being used as electrode of electrochromic supercapacitors and the stability of e-WO_3 is good.

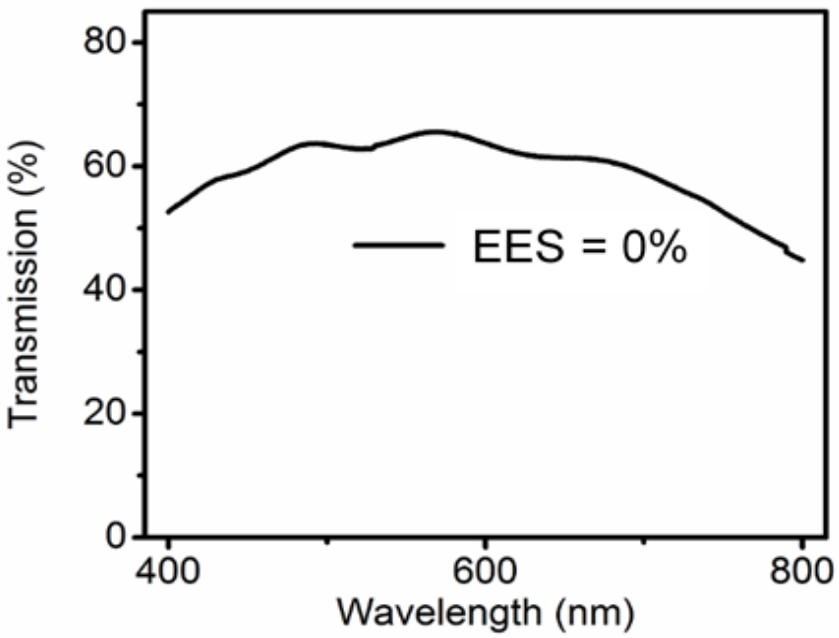

Figure S4. Transmission between 400nm and 800nm measured at the SOC=0%.

Figure S4 shows the transmission of the e-WO_3 based electrodes when the EES is 0%.

Table S3. Value of EES obtained from different plots.

Charging and discharging rate	Electrical Energy Storage (EES)				
0.05mA cm^{-2} *	18%	36%	54%	72%	90%
0.1 mA cm^{-2} #	16%	34%	53%	72%	90%

Note *: The value of normalized optical density is calculated from the fitted equation: Normalized optical density = 0.31× EES - 1.32.

Note #: The EES obtained from the fitted line in Figure 5b (charging and discharging rate: 0.1 mA cm^{-2}) is calculated from the fitted equation: Normalized optical density = 0.30 × EES - 0.46 by using the normalized optical density from the fitted line in Figure 5a (charging and discharging rate: 0.05 mA cm^{-2}).

Table S3 shows the difference of EES obtained from the two fitted curves. It can be clearly seen that the difference between EES at two charging and discharging rate is less than 2%, indicating the perfect accuracy at any charging and discharging rates by normalized optical density.

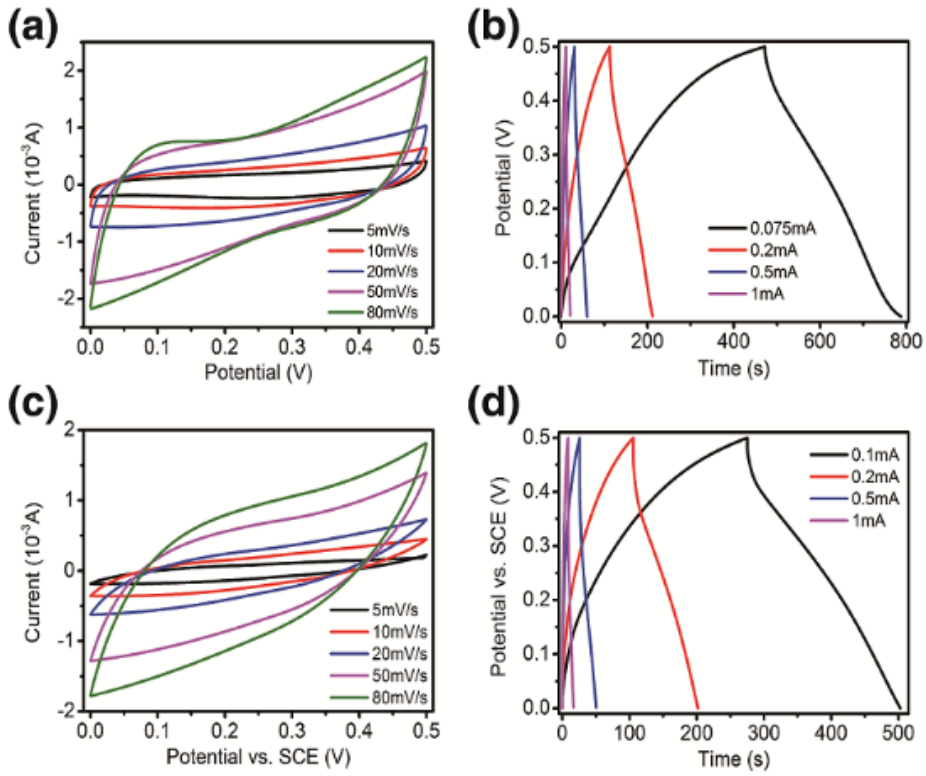

Figure S5. (a) Cyclic voltammetric and (b) galvanostatic curves of e-WO_3//PPy hybrid supercapacitors, (c) cyclic voltammetric and (d) galvanostatic curves of e-WO_3//MnO_2 hybrid supercapacitors.

Figure S5 a and b shows the cyclic voltammetric (CV) and galvanostatic curves of e-WO_3//PPy hybrid supercapacitors measured at different scan rates and charging/discharging currents. Evidently, the distortion of CV curves from ideal capacitive behavior can be found which results from the involved redox reaction. However, the CV curves are relatively symmetrical, indicating the good reversibility. The galvanostatic curves also exhibits the characteristic pseudocapacitive behavior – distortion from the ideal triangle but the good symmetric shape. Figure S5 c and d shows the CV curves and galvanostatic curves of e-WO_3//MnO_2 hybrid supercapacitors measured at different scan rates and charging/discharging currents. The distortion of CV curves are severer than that

of the e-WO_3//PPy hybrid supercapacitors due to the limited conductivity of MnO_2. However, the CV and galvanostatic curves of e-WO_3//MnO_2 also exhibits the typical pseudocapacitive behaviors.

References:

[1] Y. Tian, S. Cong, W. Su, H. Chen, Q. Li, F. Geng, Z. Zhao, Nano Lett. 14 (2014) 2150-2156.

[2] H. Wei, X. Yan, S. Wu, Z. Luo, S. Wei, Z. Guo, J. Phys. Chem. C 116 (2012) 25052-25064.

[3] P. Yang, P. Sun, Z. Chai, L. Huang, X. Cai, S. Tan, J. Song, W. Mai, Angew. Chem. Int. Ed.126 (2014) 12129-12133.

[4] Z. Xie, X. Jin, G. Chen, J. Xu, D. Chen, G. Shen, Chem. Commun. 50 (2013) 608-610.